



Triangle-shaped polycyclic aromatics based on tribenzocoronene: facile synthesis and physical properties

Zhongtao Li^a, Linjie Zhi^b, Nigel T. Lucas^c, Zhaohui Wang^{a,*}

^aKey Laboratory of Organic Solids, Institute of Chemistry, Chinese Academy of Sciences, Beijing 100080, PR China

^bNational Center for Nanoscience and Technology of China, Beijing 100080, PR China

^cSchool of Chemistry, The University of Sydney, NSW 2006, Australia

ARTICLE INFO

Article history:

Received 15 October 2008

Received in revised form 6 February 2009

Accepted 17 February 2009

Available online 25 February 2009

Keywords:

Polycyclic aromatics

Packing arrangement

Synthesis

Physical properties

ABSTRACT

A series of triangle-shaped polycyclic aromatics have been developed according to a facile synthetic protocol with high yields. As revealed by X-ray single crystal data, their molecular conformation and packing arrangement are significantly influenced by the electronic properties and steric bulk of peripheral subunits. The 'saddle'-shaped hexahalotribenzocoronenes (CITBC and FTBC) possess C_2 symmetric structures and can self-assemble into well-defined columnar structures, dramatically different from hexabutyxytribenzocoronene (TBC), which adopts a C_3 symmetric 'double-concave' structure and less efficient packing arrangement. In the compound trithiophenocoronene (TTC), the five-membered corner rings produce a more open bay-region periphery alleviating intramolecular steric congestion. As a result, the molecule adopts an almost planar conformation.

© 2009 Elsevier Ltd. All rights reserved.

1. Introduction

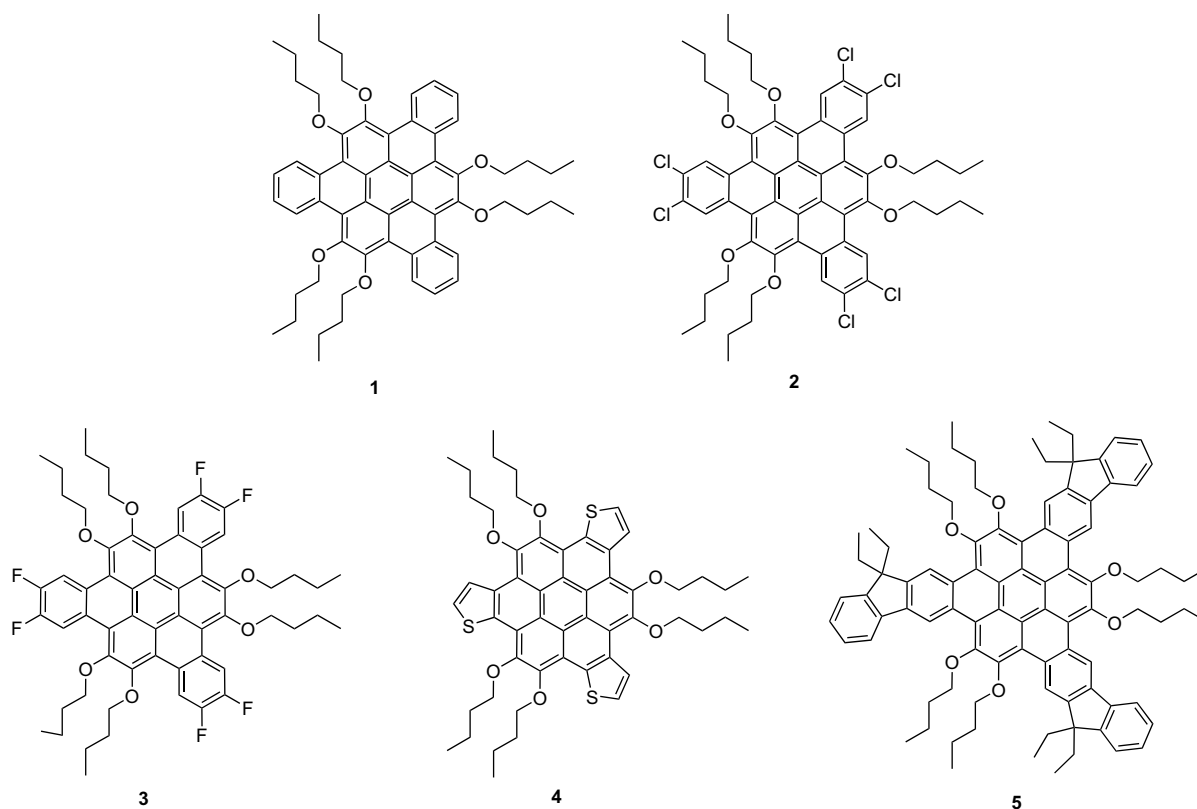
Over the last few decades, increasing attention has been paid to polycyclic aromatic hydrocarbons (PAHs), as they have been successfully used as functional materials for organic photonic and electronic devices such as field-effect transistors (FETs), light-emitting diodes (OLEDs), and solar cells.¹ The C_3 symmetric aromatic compounds, such as triphenylene and truxene derivatives, represent an intriguing PAH family. They are typically composed of highly-symmetric, rigid aromatic cores substituted with long alkyl chains, exhibiting liquid crystalline properties and charge-transport capabilities.² Recently reported, triangle-shaped molecules with C_3 symmetry, regarded as bowl-shaped subunits of fullerenes, have drawn the attention of synthetic chemists. However, the complicated synthetic procedures and the difficulty of chemical modification limit these molecules from being further investigated in a range of applications.³ In comparison, we have developed a facile approach toward triangular triarocoronenes (TACs), and two derivatives of coronene with extended core structures, hexabutoxytribenzo[*a,g,m*]coronene **1** (TBC) and hexachlorotribenzocoronene **2** (CITBC)⁴ have thus far been reported.

It is known that PAHs tend to self-assemble into columnar motifs due to the strong aromatic interaction between the PAHs.⁵

The aromatic structure together with the functional groups at the periphery of the PAHs exhibits significant influence on the stacking behavior of the molecules, which in turn influences the physical properties of the materials.^{3a,6} For example, compounds **1** and **2** have the same core structure but different functional groups at the vertices. The twist of the aromatic core into a non-planar conformation is clearly due to the extension of coronene into a triangle-shaped core structure. Variation of the functional groups between **1** and **2** results in different solid-state conformations, dubbed 'double-concave' and 'saddle-shaped', respectively. The core topography is expected to affect the aggregation behavior of these two compounds.

To better understand the relationship between molecular properties and functional groups in the peripheral regions, further functionalization of **1** is necessary. Firstly, the electron-withdrawing effect of chlorine in **2** is thought to be one of the main reasons for the dramatically changed molecular properties. Thus, fluorine, which is a stronger electron acceptor, would be expected to play a greater role in stabilizing the molecular energy although the synthesis of highly fluorinated arenes is always a challenging subject in synthetic chemistry.⁷ Secondly, increasing attention has been focused on heterocyclic PAHs, especially those containing thiophene units,^{1e,8} and upon heteroatom incorporation the aromatic behavior of the PAHs is impacted.⁹ At the same time, the thiophene ring has a smaller π conjugated system than that of benzene, and the absence of associated hydrogen atoms at the site of sulfur would alleviate the steric congestion of **1** and **2**. In

* Corresponding author. Tel./fax: +86 010 62650811.
E-mail address: wangzhaohui@iccas.ac.cn (Z. Wang).



addition, further extension of the triangle-shaped core structure by using, for instance, fluorene units at the vertices would lead to not only an enlarged core section but alternation of the aromatic area of the PAHs. As a chromophore, the fluorene units in the core would also enhance the energy transfer behavior of the molecules.

Herein, we report the design and successful syntheses of a series of triangular TACs (Scheme 1) with different cores and peripheral substitution, namely a hexafluorotribenzo[*a,g,m*]coronene **3** (FTBC), a trithiopheno[*a,g,m*]coronene **4** (TTC), and a tris(diethylfluoreno)[*a,g,m*]coronene **5** (TFC), to further unravel the structure–property relationships of the TAC derivatives. Their crystalline structures, aggregation behavior in solution, photophysical and electronic properties are discussed.

2. Results and discussion

2.1. Synthesis

Substituted triphenylenes are traditional discotic liquid crystal materials and can be easily synthesized on a gram-scale. Compound **3** was synthesized in moderate yield via bromination of hexabutoxytriphenylene,¹⁰ followed by palladium-mediated Suzuki cross-coupling of **6** with boronic acid **10** and subsequent intramolecular oxidative cyclodehydrogenation with ferric chloride.¹¹ Compounds **4** and **5** were prepared following a similar procedure; palladium-catalyzed cross-coupling of **6** with readily accessed boronic acid **11**¹² or ester **12**¹³ afforded compounds **8** (83%) and **9** (76%) in high yields, respectively. Oxidative dehydrogenation of compounds **8** and **9** with FeCl₃ gave the desired products **4** and **5** in 47% and 58% yield, respectively. No more than 6 equiv of FeCl₃ should be used, otherwise side products will be

produced as the α sites of thiophene ring, and the 2 and 7 positions of the fluorene unit have high activity in the presence of FeCl₃.

2.2. ¹H NMR spectroscopy

The ¹H NMR spectrum of compound **3** in CDCl₃ displays five highly resolved signals, which show no significant change upon cooling to 223 K, indicative of a homogeneous and symmetric proton environment. The spectra of **4** and **5** are more complicated due to their lower symmetry. The ¹H NMR spectrum of compound **4** at room temperature in CDCl₃ shows doublets at 9.72 ppm and 7.95 ppm corresponding to the core proton environments, two multiplet signals of equal integration for the O–CH₂ protons, broadly divided between methylene groups closer to the sulfur of the thiopheno-group, and those closer to the hydrogen in the 4-position. The six hydrogens of the tribenzocoronene core of **5** are all inequivalent and appear as singlets between 10.06 ppm and 9.65 ppm, while the outer hydrogens of the fluorenyl fragments appear upfield at 8.00 and 7.44 ppm. Likewise for **4**, the O–CH₂ protons of **5** are observed in two regions, at 4.32 ppm and 4.17 ppm, based on neighboring group influences.

2.3. Single-crystal structural analysis

To better understand the nature of these molecules and their intermolecular interactions, single crystals of compounds **3** and **4** were grown by slow evaporation of acetone solutions at room temperature. Crystallographic data are given in the [Experimental section](#), and the complete information is provided in the [Supporting Information](#).

The crystal structure of FTBC **3** is shown in [Figure 1](#). As illustrated in [Figure 1a](#), the fused core of **3** adopts a non-planar ‘saddle’ shape,

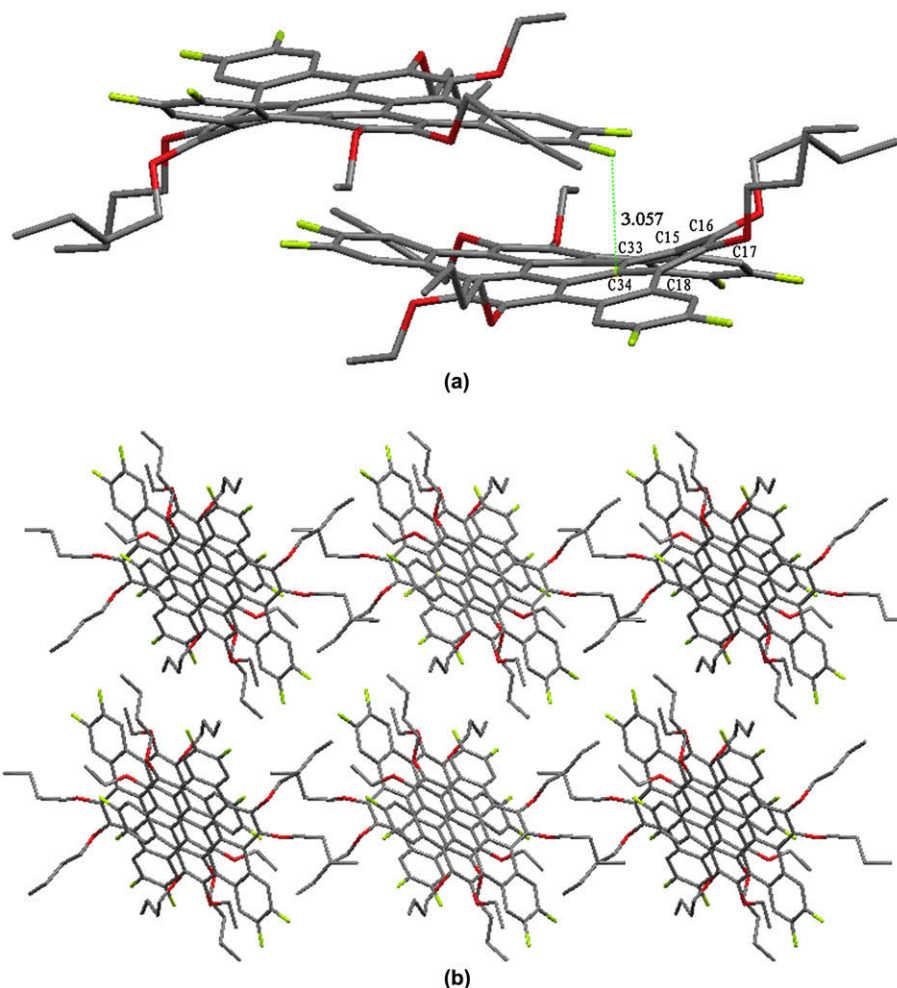


Figure 1. Crystal structure of **3**: (a) a pair of π - π interacting molecules; (b) crystal packing viewed down the b -axis.

the central coronene core. In the case of TBC **1**, only a one ring overlap is observed. The calculated face-to-face distance between the two molecules of **4** is 3.26 Å, somewhat shorter than the corresponding distance in many other π -stacking materials,¹⁴ suggesting a very strong π - π interaction. The introduction of smaller thiophene rings (compared to benzene ring) at the periphery of TTC seems to not only eliminate the molecular steric congestion, but also plays an important role in stabilizing the conjugated area of the molecule. The hydrogen atom in the 4-position of each thiopheno ring is involved in weak intramolecular hydrogen bonding with the closest alkoxy oxygen atom, but there is no sign of hydrogen-bonding participation by the thiopheno sulfur atoms. A columnar structure is built up from dimers stacked along the b -axis of the crystal (Fig. 2b). Between the dimer pairs the π - π stacking is somewhat weaker than that in intra-dimer. Only one thiopheno ring and two benzo rings overlap with each other between the neighboring dimers. Close S...S contacts appear to play no role in columnar or intercolumnar organization, which is dominated by van der Waals interactions between the alkyl chains.

2.4. Photophysical properties

All the TACs are soluble in common organic solvents such as chloroform and toluene. The optical absorption spectra of **1–5** in chloroform at room temperature are shown in Figure 3.

The UV-vis absorption spectrum of FTBC **3** shows a maximum absorbance at 348 nm ($\epsilon=108\,000\text{ M}^{-1}\text{ cm}^{-1}$), which is hypsochromically shifted 13 nm compared with that of CITBC **2** (361 nm), providing further evidence that substitution affects the properties of the TBCs. One can speculate that the stronger electron-withdrawing ability and weaker p- π conjugation of the six fluorine atoms compared with chlorine decreases the size of the conjugated π system of the TBC core, resulting in a blue shift on moving from **2** to **3**. It should be noted that the absorption of **3** in toluene or chloroform is concentration independent (in the range of 10^{-6} to 10^{-4} M) and follows the Beer-Lambert law, indicating that no aggregation takes place in solution under these conditions. These results, together with the C_3 symmetry of **3** in solution as shown by ^1H NMR indicate that the 'saddle-shaped' structure with strong intermolecular interactions may only exist in the crystalline solid state.

The spectrum of **4** shows a sharp band with a maximum absorbance at 350 nm ($\epsilon=172\,000\text{ M}^{-1}\text{ cm}^{-1}$), comparable in energy with that of TBC **1**. In contrast, the maximum absorbance of **5** shifts bathochromically to 373 nm ($\epsilon=132\,000\text{ M}^{-1}\text{ cm}^{-1}$), consistent with the larger conjugated π system of the molecule. Compounds **1–3** each display two absorption maxima but the lower symmetry **4** and **5** have five (330, 350, 375, 383, and 401 nm) and four (333, 373, 400, and 420 nm) maxima, respectively. The fluorescence quantum yield of compound **4** is just 0.053, which is the lowest of all known TACs. It may be that as **4** is the only strictly planar molecule, and

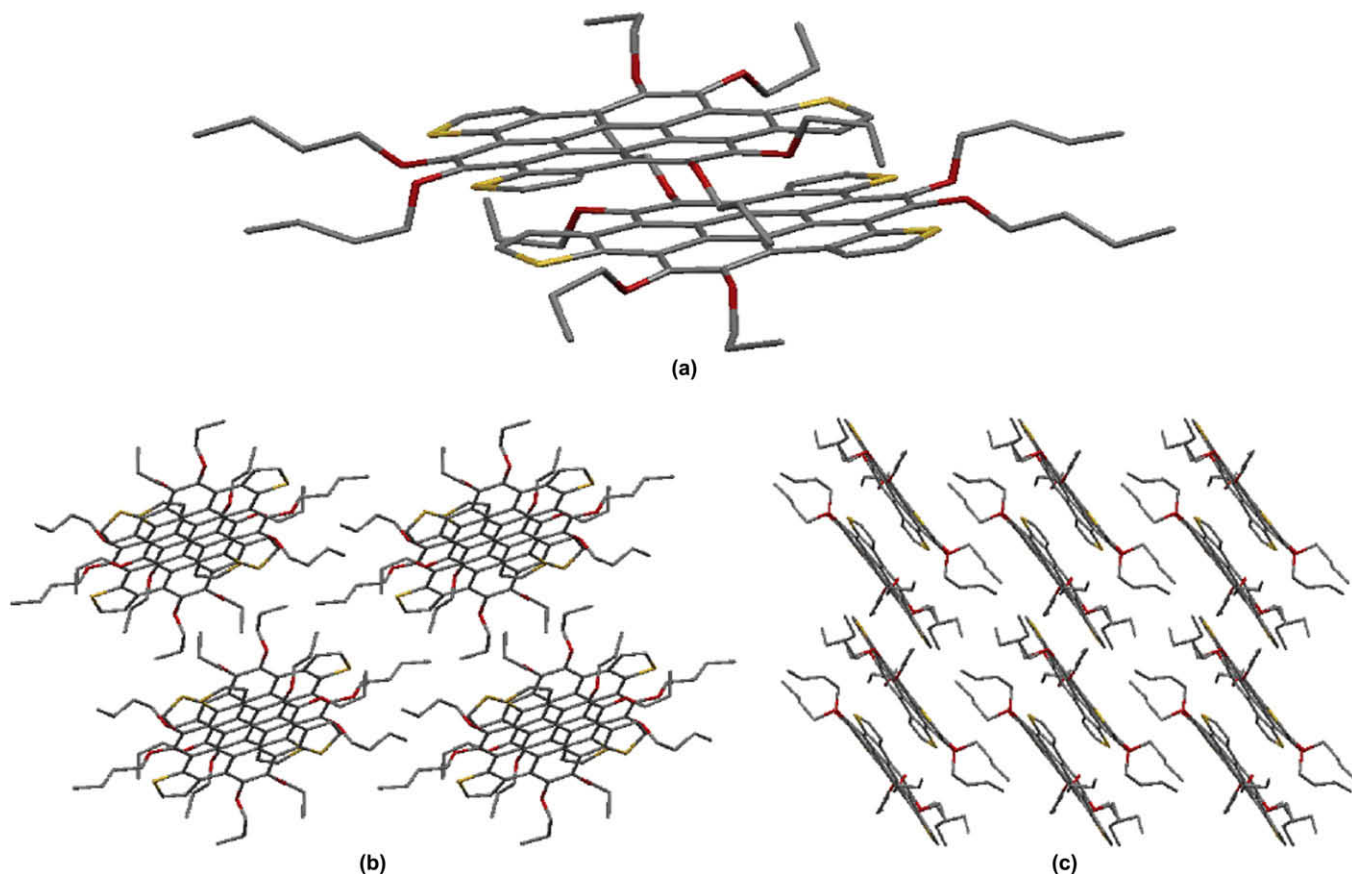


Figure 2. Crystal structure of **4**: (a) a pair of π - π interacting molecules, (b) molecular packing viewed down the b -axis. (c) Molecular packing viewed down the c -axis.

strong intramolecular interactions of **4** enhance its charge-transport properties, leading to high fluorescence quenching. The TAC **5** has the highest quantum yield of 0.26. The fluorenyl groups annulated at the periphery, regarded as a luminescent region, would likely enhance the luminescent efficiency of the molecule. In addition, the steric congestion at the edges would render the molecule non-planar, reducing intermolecular energy transfer.

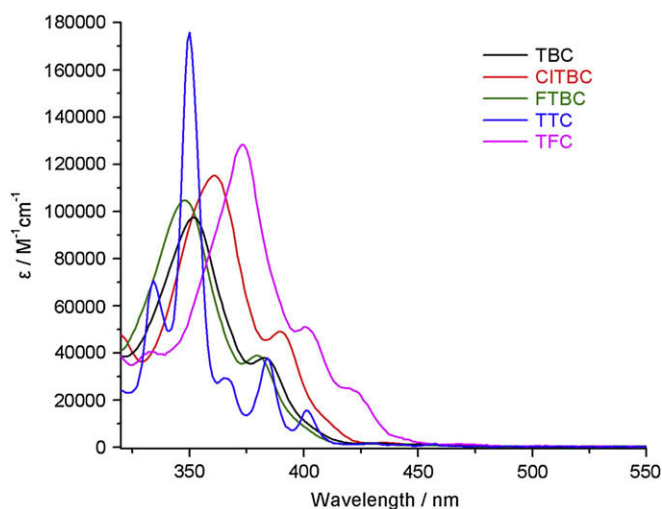


Figure 3. Absorption spectra of TBC **1** (dark line), CITBC **2** (red line), FTBC **3** (olive line), TTC **4** (blue line) and TFC **5** (magenta line) at 10^{-6} M in chloroform.

2.5. Electronic properties

To elucidate the influence of various peripheral functional groups of the TACs on the molecular energy levels, the HOMO values of compounds **1–5** were obtained in dilute solution via cyclic voltammetry measurements. The measurements were carried out at a glassy carbon microelectrode in CH_2Cl_2 (0.1 M $[\text{nBu}_4][\text{PF}_6]$ electrolyte; Ag/AgNO_3 reference electrode). Each measurement was internally calibrated against ferrocene (Fc), $E^{\text{Fc}}_{1/2} = -0.162$ V versus Ag/AgNO_3 .¹⁵ All data are listed in Table 1.

The parent TBC, **1** shows two well-resolved reversible oxidations at 1.00 V and 1.26 V versus Ag/Ag^+ , which results in a HOMO value of -5.64 eV (on the basis of the HOMO energy level of Ag/Ag^+ as -4.64 eV). In comparison, the introduction of six chlorines at the periphery leads to an anodic shift of the oxidation states to 1.10 V and 1.32 V, respectively for **2**. This shift is explained by the electron-withdrawing effect of the chlorine atoms, supported by a further anodic shift for the fluorinated analog; the oxidation potentials of FTBC **3** are observed at 1.22 V and 1.45 V, respectively. The electron-rich groups of **4** and **5** increase the ease of oxidation, showing peaks

Table 1

Cyclic voltammetry of compounds **1–5** in CH_2Cl_2 (0.1 M $[\text{nBu}_4\text{N}][\text{PF}_6]$) at a GC working electrode at a scan rate of 0.1 V s^{-1}

Compound	E_{ox1} (V)	E_{ox2} (V)	HOMO (eV)
1	1.00	1.26	-5.64
2	1.10	1.32	-5.74
3	1.22	1.45	-5.86
4	0.87	1.29	-5.51
5	0.88	1.21	-5.52

at 0.87 V/1.29 V and 0.88 V/1.21 V, respectively, cathodically shifted compared to **1**. These results illustrate the strong correlation between the electron richness of the TAC core and its oxidizability, and that tuning of the redox properties may be effected by peripheral substitution in combination with core expansion (as in the case of **5**). Within the series of TACs presented here the HOMO energy spans the range -5.51 eV (**4**, S-containing core) to -5.86 eV (**3**, fluorine-substitution).

3. Conclusion

Three new compounds, **3–5**, with trigonally extended coronene core structures and enlarged aromatic π systems, have been successfully synthesized in good yield via oxidative cyclodehydrogenation of a triarotriphenylene precursor. Further investigation indicates that the halogen substitution seems to have a significant effect on the molecular structure and physical properties of these compounds. Single-crystal X-ray structure analysis reveals that stronger intramolecular solid-state interactions result from incorporation of electron-withdrawing halogen substituents, consistent with a higher melting point for the fluoro-bearing **3** compared with its chloro analog **2**. The cyclic voltammetry data reveal that the strong electron-accepting nature of the substituents produces an anodic shift of oxidation processes. Other aromatic systems at the periphery such as thiophene and fluorene also significantly modify the molecular characteristics. The smaller size of the thiophene ring eliminates steric congestion, leading to a planar conformation. Optical studies indicate that **4** and **5** both have additional absorption peaks compared to **1–3**, ascribed to the lower symmetry of the molecules. As electron donating moieties, the thiophene and fluorene subunits render the core electron rich and molecular HOMO energy levels are lower than in the other TACs. Ongoing work will address the incorporation of other functional components at the periphery of the PAH to enable further tuning of the structural, optoelectronic, and material properties of these functional materials.

4. Experimental section

4.1. General techniques

^1H NMR and ^{13}C NMR spectra were recorded in deuteriochloroform (CDCl_3) with a Bruker DMX 300 MHz NMR or a Bruker DMX 400 MHz NMR spectrometer. J values are expressed in hertz and quoted chemical shifts are in parts per million. Splitting patterns are indicated as s, singlet; d, doublet; t, triplet; q, quartet, m, multiplet. Ultraviolet and visible spectra were recorded on a Hitachi U-3010 UV–Vis spectrophotometer. Melting points were measured using hot stage microscope, and are uncorrected. The X-ray diffraction data were collected on Rigaku Saturn diffractometer with CCD area detector. All calculations were performed using the SHELXL97 and CrystalStructure crystallographic software packages. Mass spectra (MALDI-TOF) were measured on a Bruker BIFLEX III Mass Spectrometer. The fluorescence quantum yield was determined by the optically dilute method with 9,10-diphenylanthracene ($\phi=1$, in cyclohexane)¹⁶ as reference. Cyclic voltammograms (CVs) were recorded on a Zahner IM6e electrochemical workstation using glassy carbon discs as the working electrode, Pt wire as the counter electrode, Ag/AgNO_3 as the reference electrode, and ferrocene/ferrocenium as an internal potential marker.

4.2. Synthetic procedures

4.2.1. 2,3,6,7,10,11-Hexabutoxy-1,4,8-tris(3,4-difluorophenyl)-triphenylene **7**

A Schlenk flask was charged with 1,4,8-tribromo-2,3,6,7,10,11-hexabutoxytriphenylene **6** (1.00 g, 1.11 mmol), tetrakis

(triphenylphosphine)palladium(0) (300 mg, 0.260 mmol), THF (75 mL), and 2 M potassium carbonate solution (25 mL) under argon, then 3,4-difluorophenylboronic acid (750 mg, 4.75 mmol) was added. The mixture was heated to 85 °C with vigorous stirring for 12 h, cooled to room temperature, and the organic phase separated and washed twice with water. After drying over magnesium sulfate and filtering, the solvent was removed in vacuo. The residue was purified by column chromatography on silica (50% petroleum ether–dichloromethane) to give **7** (810 mg, 0.81 mmol, 73%) as a white solid. ^1H NMR (CDCl_3 , 400 MHz): δ 7.78–7.35 (m, 2H), 7.25 (s, 2H), 7.20 (s, 6H), 6.85 (s, 1H), 6.78 (s, 1H), 4.12–3.26 (m, 12H), 1.62 (m, 6H), 1.38 (m, 12H), 1.16 (m, 6H), 0.96 (m, 9H), 0.76 (m, 9H). ^{13}C NMR (CDCl_3 , 100 MHz): δ 149.6, 149.5, 149.1, 146.2, 146.0, 145.6, 136.8, 130.5, 130.0, 129.4, 128.8, 127.7, 126.9, 124.5, 123.9, 113.2, 112.4, 76.7, 72.6, 67.9, 32.3, 32.2, 31.2, 31.0, 19.1, 13.7. Elemental analysis calcd for $\text{C}_{60}\text{H}_{66}\text{F}_6\text{O}_6$: C, 72.27; H, 6.67; found: C, 71.97; H, 6.63. MALDI-TOF (m/z): calcd for $\text{C}_{60}\text{H}_{66}\text{F}_6\text{O}_6$ 996.5, found 997.1. Mp 80–82 °C.

4.2.2. 1,2,7,8,13,14-Hexabutoxy-4,5,10,11,16,17-hexafluorotribenzo[*a,g,m*]coronene **3**

To a solution of 2,3,6,7,10,11-hexabutoxy-1,4,8-tris(3,4-difluorophenyl)triphenylene **7** (810 mg, 0.81 mmol) in dichloromethane (50 mL) was added ferric chloride (1.58 g, 9.7 mmol) in 2 mL of nitromethane. The mixture was stirred for 20 min at room temperature. To quench the reaction, methanol (20 mL) was added, then 30 mL of water. The organic layer was separated and the solvent removed in vacuo. The residue was purified by column chromatography on silica (50% petroleum ether–dichloromethane) and recrystallization of the major product from hexane afforded **3** as yellow needles (224 mg, 0.227 mmol, 28%). ^1H NMR (CDCl_3 , 400 MHz): δ 9.75 (t, $J(\text{F,H})=11.8$ Hz, 6H), 4.23 (t, $J=6.67$ Hz, 12H), 2.04 (m, 12H), 1.69 (m, 12H), 1.07 (t, $J=7.3$ Hz, 18H). ^{13}C NMR (CDCl_3 , 100 MHz): δ 149.5, 128.7, 127.1, 126.7, 121.7, 120.6, 74.7, 32.9, 19.9, 14.4. Elemental analysis calcd for $\text{C}_{60}\text{H}_{60}\text{F}_6\text{O}_6$: C, 72.71; H, 6.10; found: C, 72.92; H, 6.31. MALDI-TOF (m/z): calcd for $\text{C}_{60}\text{H}_{60}\text{F}_6\text{O}_6$ 990.0, found 990.1. Mp 231–232 °C.

4.2.3. 3-(2,3,6,7,10,11-Hexabutoxy-1,5-di(thiophen-3-yl)triphenylene-8-yl)thiophene **8**

A Schlenk flask was charged with 1,4,8-tribromo-2,3,6,7,10,11-hexabutoxytriphenylene **6** (1.00 g, 1.11 mmol), tetrakis(triphenylphosphine)palladium(0) (300 mg, 0.260 mmol), THF (75 mL), and 2 M potassium carbonate solution (25 mL) under argon, then thiophen-3-ylboronic acid (710 mg, 5.6 mmol) was added. The mixture was heated to 85 °C with vigorous stirring for 12 h, cooled to room temperature, and the organic phase separated and washed twice with water. After drying over magnesium sulfate, the solvent was removed in vacuo. The residue was purified by column chromatography on silica (50% petroleum ether–dichloromethane) to give **8** (840 mg, 0.93 mmol, 83%) as a white solid. The product is somewhat sensitive to air, darkening over days. ^1H NMR (CDCl_3 , 400 MHz): δ 7.43 (m, 3H), 7.34 (m, 3H), 7.22 (s, 1H), 7.18 (s, 2H), 7.06 (s, 2H), 6.97 (s, 1H), 3.7 (s, 4H), 3.53 (t, $J=7.3$ Hz, 2H), 3.47–3.37 (m, 6H), 1.65 (m, $J=7.8$ Hz, 6H), 1.41 (m, $J=7.5$ Hz, 12H), 1.20 (m, $J=7.1$ Hz, 6H), 0.94 (m, 9H), 0.78 (m, 9H). ^{13}C NMR (CDCl_3 , 100 MHz): δ 149.9, 149.6, 146.0, 139.5, 139.3, 139.1, 131.3, 130.9, 129.2, 128.2, 127.5, 126.2, 125.6, 125.0, 124.6, 124.4, 124.2, 111.8, 111.4, 111.2, 73.3, 72.6, 67.6, 67.3, 32.4, 31.2, 19.2, 13.9. Elemental analysis calcd for $\text{C}_{54}\text{H}_{66}\text{O}_6\text{S}_3$: C, 71.49; H, 7.33; found: C, 71.58; H, 6.61. MALDI-TOF (m/z): calcd for $\text{C}_{54}\text{H}_{66}\text{O}_6\text{S}_3$ 907.3, found 906.4. Mp 52–55 °C.

4.2.4. 1,2,7,8,13,14-Hexabutoxytrithiopheno-[*a*:2,3;*g*:2,3;*m*:3,2]-coronene **4**

To a solution of **8** (840 mg, 0.93 mmol) in dichloromethane (150 mL) was added ferric chloride (900 mg, 5.58 mmol) in 2 mL of

nitromethane. The mixture was stirred for 20 min at room temperature, before being quenched with methanol (30 mL), then 30 mL water. The organic layer was separated and the solvent removed in vacuo. The residue was purified by column chromatography on silica (50% petroleum ether–dichloromethane) and recrystallization of the major product from acetone afforded **4** as a yellow dust (400 mg, 0.44 mmol, 47%). ¹H NMR (CDCl₃, 300 MHz): δ 9.35 (d, *J*=5.3 Hz, 3H), 8.00 (d, *J*=5.3 Hz, 3H), 4.67 (m, 6H), 4.53 (m, 6H), 2.33 (tt, *J*=6.5 Hz, 6H), 2.19 (tt, *J*=6.7 Hz, 6H), 1.70 (m, 12H), 1.12 (m, 12H). ¹³C NMR (CDCl₃, 100 MHz): δ 148.5, 148.4, 147.6, 145.5, 134.1, 133.7, 128.0, 127.5, 122.0, 121.8, 121.7, 121.6, 121.5, 120.9, 120.7, 77.6, 33.5, 20.4, 15.2. Elemental analysis calcd for C₅₄H₆₀O₆S₃: C, 71.97; H, 6.71; found: C, 72.03; H, 6.36. MALDI-TOF (*m/z*): calcd for C₅₄H₆₀O₆S₃ 901.2, found 900.8. Mp 172–174 °C.

4.2.5. 2,3,6,7,10,11-Hexabutoxy-1,4,8-tris(9,9-diethyl-9H-fluorenyl)triphenylene **9**

A Schlenk flask was charged with 1,4,8-tribromo-2,3,6,7,10,11-hexabutoxytriphenylene **6** (1.00 g, 1.11 mmol), tetrakis(triphenylphosphine)palladium(0) (300 mg, 0.260 mmol), THF (75 mL), and 2 M potassium carbonate solution (25 mL) under argon, then 2-(9,9-diethyl-9H-fluorenyl)-4,4,5,5-tetramethyl-1,3,2-dioxaborolane (2.0 g, 5.5 mmol) was added. The mixture was heated to 85 °C with vigorous stirring for 12 h, cooled to room temperature, and the organic phase separated and washed twice with water. After drying over magnesium sulfate, the solvent was removed in vacuo. The residue was purified by column chromatography on silica (50% petroleum ether–dichloromethane) to give **9** (1.11 g, 0.84 mmol, 76%) as a pale yellow solid. ¹H NMR (CDCl₃, 400 MHz): δ 7.96–7.51 (m, 9H), 7.31 (s, 6H), 7.13–6.85 (m, 3H), 4.05–2.86 (m, 12H), 1.88–1.82 (m, 10H), 1.51–1.08 (m, 32H), 0.73–0.63 (m, 18H), 0.28–0.12 (m, 12H). ¹³C NMR (CDCl₃, 75 MHz): δ 150.5, 150.3, 150.0, 149.7, 149.3, 145.7, 145.6, 141.3, 141.1, 140.1, 139.9, 133.1, 127.8, 126.8, 122.9, 119.5, 119.3, 73.3, 72.5, 67.7, 67.2, 56.3, 56.2, 56.0, 32.9, 32.7, 32.3, 31.9, 31.1, 30.8, 30.7, 19.0, 18.9, 18.8, 13.7, 13.6, 13.4, 8.6, 8.2. Elemental analysis calcd for C₉₃H₁₀₈O₆: C, 84.50; H, 8.24; found: C, 84.19; H, 8.07. MALDI-TOF (*m/z*): calcd for C₉₃H₁₀₈O₆ 1321.2, found 1322.1. Mp 47–49 °C.

4.2.6. 1,2,7,8,13,14-Hexabutoxy-tri(9,9-diethylfluoreno)-[a:2,3;g:2,3;m:3,2]coronene **5**

To a solution of **9** (1.11 g, 0.84 mmol) in dichloromethane (150 mL) was added ferric chloride (820 mg, 5.0 mmol) in 2 mL of nitromethane. The mixture was stirred for 20 min at room temperature, before being quenched with methanol (30 mL), then 30 mL water. The organic layer was separated and the solvent removed in vacuo. The residue was purified by column chromatography on silica (50% petroleum ether–dichloromethane) and recrystallization of the major product from acetone afforded **5** as a dark green solid (640 mg, 0.49 mmol, 58%). ¹H NMR (CDCl₃, 300 MHz): δ 10.09 (s, 1H), 10.06 (s, 1H), 10.02 (s, 1H), 9.73 (s, 1H), 9.69 (s, 1H), 9.65 (s, 1H), 8.00 (t, *J*=6.2 Hz, 3H), 7.44 (t, *J*=5.8 Hz, 9H), 4.32 (q, *J*=6.5 Hz, 6H), 4.17 (q, *J*=6.7 Hz, 6H), 2.30 (m, 12 H), 2.12 (m, 12H), 1.76 (dd, *J*=5.3 Hz, 6H), 1.57 (m, 6H), 1.01 (t, *J*=6.8 Hz, 18H), 0.41 (m, 18H). ¹³C NMR (CDCl₃, 75 MHz): δ 150.9, 149.7, 149.5, 149.3, 149.0, 142.3, 141.3, 129.0, 128.8, 127.8, 127.5, 123.4, 123.1, 122.8, 121.5, 121.3, 120.4, 118.7, 74.5, 56.9, 33.9, 33.2, 19.8, 14.9, 9.0. Elemental analysis calcd for C₉₃H₁₀₂O₆: C, 84.89; H, 7.81; found: C, 85.13; H, 8.20. MALDI-TOF (*m/z*): calcd for C₉₃H₁₀₂O₆ 1313.2, found 1312.7. Mp 132–135 °C.

4.3. X-ray diffraction analyses of compounds **3** and **4**

Crystal data for 3: C₆₀H₆₀F₆O₆, *M*=991.08, yellow block, space group *P*2₁/*c*, *a*=13.5976(19), *b*=12.0988(16), *c*=29.798(4) Å, β=95.010(3)°, *Z*=4, *T*=113(2) K, *V*=4883.4(12) Å³, *D*_c=1.348 g/cm³,

μ=0.101 mm⁻¹, λ=0.71070 Å, θ_{min}=1.37°, θ_{max}=26°, crystal dimensions=0.26×0.24×0.20 mm. 39371 Reflections were scanned and [*R*_{int}=0.0520] into a unique set of 9580 reflections [7990 of which with *I*>2σ(*I*)]. The structure was solved by direct methods (SIR97) and refined on *F*² using SHELXL97. Hydrogen atoms were introduced at calculated positions and refined riding on their carrier atoms. The displacement parameters for the C₆₀ atoms display the common flat disk characteristics. Convergence was reached at *R*₁=0.0751, *wR*₂=0.1583, *S*=1.125, 9580 reflections, 687 parameters, 36 restraints, −0.418<*Δ*_r<1.104 e Å⁻³.

Crystal data for 4: C₅₄H₆₀O₆S₃, *M*=901.20, colorless prism, space group *P*−1, *a*=11.9913(12), *b*=12.1804(14), *c*=17.8243(18) Å, α=66.699(8)°, β=74.285(9)°, γ=87.656(10)°, *Z*=2, *T*=113(2) K, *V*=2295.2(4) Å³, *D*_c=1.304 g/cm³, μ=0.213 mm⁻¹, λ=0.71070 Å, θ_{min}=2.5°, θ_{max}=25°, crystal dimensions=0.32×0.24×0.12 mm. 28976 Reflections were scanned and [*R*_{int}=0.0396] into a unique set of 10822 reflections [8401 of which with *I*>2σ(*I*)]. The structure was solved by direct methods (SIR97) and refined on *F*² using SHELXL97. Hydrogen atoms were introduced at calculated positions and refined riding on their carrier atoms. The displacement parameters for the C₆₀ atoms display the common flat disk characteristics. Convergence was reached at *R*₁=0.0691, *wR*₂=0.1289, *S*=1.04, 10822 reflections, 723 parameters, 111 restraints, −0.448<*Δ*_r<0.382 e Å⁻³.

Further details of crystal structure including final atomic parameters have been deposited in the Cambridge Crystallographic Data Centre (deposition numbers: CCDC 672284 (**3**); 672285 (**4**)). Copies of the data can be obtained, free of charge, on application to CCDC, 12 Union Road, Cambridge CB2 1EZ, UK (fax: +44-(0)1223-336033 or e-mail: deposit@ccdc.cam.ac.uk).

Acknowledgements

For financial support of this research, we thank the National Natural Science Foundation of China (Grant 20772131), 973 Program (Grant 2006CB932101, 2006CB806200), and Chinese Academy of Sciences. The Australian Research Council is thanked for financial support and the award of an Australian Postdoctoral Fellowship to N.T.L.

Supplementary data

Supplementary data associated with this article can be found in the online version, at doi:10.1016/j.tet.2009.02.042.

References and notes

- (a) Clar, E. *Polycyclic Hydrocarbons*; Academic: London, 1964; For recent reviews: (b) Watson, M. D.; Fechtenkötter, A.; Müllen, K. *Chem. Rev.* **2001**, *101*, 1267; (c) Grimmsdale, A. C.; Müllen, K. *Angew. Chem., Int. Ed.* **2005**, *44*, 5592; (d) Bendikov, M.; Wudl, F.; Perepichka, D. F. *Chem. Rev.* **2004**, *104*, 4891; (e) Katz, H. E.; Bao, Z.; Gilat, S. L. *Acc. Chem. Res.* **2001**, *34*, 359.
- (a) Cammidge, A. N.; Bushby, R. J. In *Handbook of Liquid Crystals*; Demus, D., Goodby, J., Gray, G. M., Spiess, H.-W., Vill, V., Eds.; Wiley-VCH: Weinheim, 1998; Vol. 2B, Chapter VII; (b) van de Craats, A. M.; Warman, J. M. *Adv. Mater.* **2001**, *13*, 130; (c) Sandeep, K.; Sanjay, K. V. *Org. Lett.* **2002**, *4*, 157; (d) Pei, J.; Wang, J. L.; Cao, X. Y.; Zhou, X. H.; Zhang, W. B. *J. Am. Chem. Soc.* **2003**, *125*, 9944.
- (a) Wu, J.; Tomović, Ž.; Enkelmann, V.; Müllen, K. *J. Org. Chem.* **2004**, *69*, 5179; (b) Duan, X.-F.; Wang, J.-L.; Pei, J. *Org. Lett.* **2005**, *7*, 4071; (c) Cao, X. Y.; Zi, H.; Zhang, W.; Pei, J. *J. Org. Chem.* **2005**, *70*, 3645; (d) Feng, X.; Wu, J.; Ai, M.; Pisula, W.; Zhi, L.; Rabe, J. P.; Müllen, K. *Angew. Chem., Int. Ed.* **2007**, *46*, 3033; (e) Yuan, M. S.; Fang, Q.; Liu, Z. Q.; Guo, J. P.; Chen, H. Y.; Xue, G.; Liu, D. S. *J. Org. Chem.* **2006**, *71*, 7858.
- Li, Z.; Lucas, N. T.; Wang, Z.; Zhu, D. J. *Org. Chem.* **2007**, *72*, 3917.
- (a) Desiraju, G. R.; Gavezotti, A. *Acta Crystallogr., B.* **1989**, *45*, 473; (b) Hunter, C. A.; Lawson, K. R.; Perkins, J.; Urch, C. J. *J. Chem. Soc., Perkin Trans. 2* **2001**, 651; (c) Cho, D. M.; Parkin, S. R.; Wason, M. D. *Org. Lett.* **2005**, *7*, 1067.
- Wang, Z.; Tomović, Ž.; Kastler, M.; Pretsch, R.; Negri, F.; Enkelmann, V.; Müllen, K. *J. Am. Chem. Soc.* **2004**, *126*, 7794.

7. (a) Ponzini, F.; Zaghera, R.; Hardcastle, K.; Siegel, J. S. *Angew. Chem., Int. Ed.* **2000**, *39*, 2323; (b) Sakamoto, Y.; Suzuki, T.; Kobayashi, M.; Gao, Y.; Fukai, Y.; Inoue, Y.; Sao, F.; Tokito, S. *J. Am. Chem. Soc.* **2004**, *126*, 8138; (c) Chen, Z.; Muller, P.; Swager, T. M. *Org. Lett.* **2006**, *8*, 273.
8. (a) Anthony, J. E. *Chem. Rev.* **2006**, *106*, 5028; (b) Cicoira, F.; Sanao, C.; Melucci, M.; Favaretto, L.; Gazzano, M.; Muccini, M.; Barbarella, G. *Adv. Mater.* **2006**, *18*, 169; (c) Curtis, M. D.; Cao, J.; Kampf, J. W. *J. Am. Chem. Soc.* **2004**, *126*, 4318.
9. Tourillon, G.; Garnier, F. J. *Electroanal. Chem.* **1982**, *135*, 173.
10. Boden, N.; Bushby, R. J.; Cammidge, A. N.; Duckworth, S.; Headdock, G. J. *Mater. Chem.* **1997**, *7*, 601.
11. Wang, Z.; Watson, M. D.; Wu, J.; Müllen, K. *Chem. Commun.* **2004**, 336.
12. Denton, T. T.; Zhang, X.; Cashman, J. R. *J. Med. Chem.* **2005**, *48*, 224.
13. Belletête, M.; Beaupré, S.; Bouchard, J.; Blondin, P.; Leclerc, M.; Durocher, G. *J. Phys. Chem. B* **2000**, *104*, 9118.
14. (a) Anthony, J. E.; Brooks, J. S.; Eaton, D. L.; Parkin, S. R. *J. Am. Chem. Soc.* **2001**, *123*, 9482; (b) Kumar, S.; Rao, D. S. S.; Prasad, S. K. *J. Mater. Chem.* **1999**, *9*, 2751; (c) Kobayashi, K.; Shimaoka, R.; Kawahata, M.; Yamanaka, M.; Yamaguchi, K. *Org. Lett.* **2006**, *8*, 2385.
15. Thelakkat, M.; Schmidt, H. W. *Adv. Mater.* **1998**, *10*, 219.
16. *Handbook of Photochemistry*, 2nd ed.; Murov, S. L., Carmichael, I., Hug, G. L., Eds.; Marcel Dekker: New York, NY, 1993.